

METHOD FOR MEASURING MINORITY AND MAJORITY CARRIER MOBILITIES IN SOLAR CELLS

D.H. Neuhaus, P.P. Altermatt, A.B. Sproul, R.A. Sinton,* A. Schenk,** A. Wang and A.G. Aberle
 Photovoltaics Special Research Centre, University of New South Wales, Sydney NSW 2052, Australia
 Ph: (+61) 2 9385 4054, Fax: (+61) 2 9385 5412, Email: d.neuhaus@student.unsw.edu.au

* Sinton Consulting Inc., 1132 Green Circle, Boulder CO 80303, USA

** Swiss Federal Institute of Technology, ISL, Gloriastr. 35, CH-8092 Zürich, Switzerland

ABSTRACT: Contactless quasi-steady-state photoconductance (QSS-PC) measurements are widely used to measure the injection level dependence of the effective excess carrier lifetime of semiconductor samples. Alternatively, quasi-steady-state open-circuit voltage (QSS- V_{oc}) measurements can be used to measure the injection level dependence of the effective excess carrier lifetime in the bulk region of a solid-state solar cell.

In this paper, we combine both methods to measure the injection level dependence of the sum of the minority and majority carrier mobilities in the bulk of a solid-state solar cell. We verify our method by means of PC-1D computer simulations and by measurements on Si solar cells. To our knowledge, our method is the first that enables the measurement of the injection level dependence of the sum of the minority and majority carrier mobilities of a doped (i.e., non-intrinsic) Si sample.

Keywords: Photoconductivity – 1: Mobility – 2: Lifetime – 3

1. INTRODUCTION

Both the open-circuit voltage V_{oc} and the light generated current density J_L of a solid-state solar cell depend strongly on the effective excess carrier lifetime τ_{eff} and the minority carrier mobility μ_{min} in the bulk region of the cell. Hence, it is of interest to develop a simple technique that allows one to simultaneously measure τ_{eff} and μ_{min} on a finished solar cell.

In this paper we present such a technique. It is based on combining the two methods of Sinton and Cuevas [1, 2], which are known as the quasi-steady-state photoconductance (QSS-PC) method and the quasi-steady-state open-circuit voltage (QSS- V_{oc}) method. These methods are commonly applied to measure the injection level dependence of the effective excess carrier lifetime $\tau_{eff}(\Delta n)$. By combining both methods, we are able to measure the injection level dependence of the sum of the minority and majority carrier mobilities $\mu_{sum}(\Delta n) \equiv \mu_{min}(\Delta n) + \mu_{maj}(\Delta n)$ in the bulk of a solid-state solar cell, *regardless* of the bulk doping density N_{Bulk} . The mobilities $\mu_{min}(\Delta n)$ and $\mu_{maj}(\Delta n)$ can then be separated using commonly used mobility models [3,4]. Beyond this, our method offers additional advantages. For example, we have only found $\mu_{sum}(\Delta n)$ measurements in the literature that were performed under high-injection, while with our method we can measure $\mu_{sum}(\Delta n)$ in the whole range from low to high injection. This is particularly useful for improving the QSS-PC method, where the injection level dependence of $\mu_{sum}(\Delta n)$ is required. So far, $\mu_{sum}(\Delta n)$ had to be assumed using an empirical model [5].

In the first part of this paper, we describe a simple set of analytical expressions that form the basis of our method. Then, we test these equations by means of numerical simulations using the semiconductor device simulator PC-1D [6]. Finally, we verify our method by measuring $\mu_{sum}(\Delta n)$ in a PERL solar cell [7] made from 0.9 Ωcm p -type FZ Si.

2. DERIVATION OF THE METHOD

Recently, Sinton and Cuevas presented a simple and

elegant quasi-steady-state photoconductance (QSS-PC) method [1] to measure $\tau_{eff}(\Delta n)$. In this method, the spatial average of the excess carrier density Δn_{av} has to be recorded for different incident light intensities. In Ref. 1 a slowly decaying flash lamp is used to generate excess carriers in a Si wafer with or without junction. The decaying Δn_{av} is then monitored indirectly by monitoring the decaying photoconductance $\Delta\sigma$ using

$$\Delta\sigma = qW\Delta n_{av}\mu_{sum}, \quad (1)$$

where q is the elementary charge, W the wafer thickness, and $\mu_{sum}(\Delta n)$ is calculated using a semi-empirical model [5]. The decaying $\Delta\sigma$ is measured with a calibrated coil inductively coupled to the free carriers in the wafer. Additionally, if the decaying Δn_{av} is measured as well, the same approach can be used to monitor $\mu_{sum}(\Delta n)$. We measure Δn_{av} with the second method introduced by Sinton and Cuevas [2], the QSS- V_{oc} technique. Again, a slowly decaying flashlight is used to generate excess carriers. The open-circuit voltage V_{oc} generated by these excess carriers is monitored via the terminals of the junction, and Δn_{av} is then calculated from V_{oc} . In particular, it is the excess carrier density at the edge of the space charge region Δn_{scr} that is calculated from V_{oc} , according to

$$(n_0 + \Delta n_{scr})(p_0 + \Delta n_{scr}) = n_{i,eff}^2 \exp\left(\frac{qV_{oc}}{kT}\right). \quad (2)$$

T is the absolute temperature and k Boltzmann's constant. The equilibrium electron and hole densities in the bulk, n_0 and p_0 , are known from the bulk dopant density. We calculate the effective intrinsic carrier density $n_{i,eff}$ by using the $n_{i,eff}$ value of $9.65 \times 10^9 \text{ cm}^{-3}$ of Ref. 8 for intrinsic Si in low injection at 300 K and by utilizing the temperature, doping and injection dependence of Ref. 13 and 14. We have $\Delta n_{scr} = \Delta n_{av}$ if (i) the minority carrier diffusion length L_{min} in the bulk is much larger than its thickness W , and (ii) the device has a low effective surface recombination velocity S_{eff} at the front and the rear surface. If these requirements are not fulfilled, we calculate Δn_{av} from Δn_{scr} using the simple analytical approximations given in Ref. 9. Note that $\Delta n_{av} \approx \Delta n_{scr}$ does not hold for very low injection

levels. This is because the component of the photoconductance arising from the space-charge region becomes larger than the component of the photoconductance arising from the bulk region of the solar cell as described in Ref. 10.

In summary, by combining the QSS-PC and the QSS- V_{oc} method, we combine their underlying equations (1) and (2) to obtain $\mu_{sum}(\Delta n)$. In the next section, we test the validity of the equations and our assumptions by simulating our experiment with PC-1D [6].

3. NUMERICAL VALIDATION OF THE METHOD

The Si solar cell structure used in our simulations is based on a 200 μm thick, 1 Ωcm p -type Si wafer with an n^+ emitter at the front and a p^+ BSF at the rear. The PC-1D simulation parameters are given in Table 1. The structure incorporates a very lightly doped and thin emitter and back-surface-field (BSF) regions and very low surface recombination velocities. At V_{oc} , these conditions guarantee a constant excess carrier density throughout the entire bulk region, which allows us to use the simple approximation $\Delta n_{av} = \Delta n_{scr}$ in our calculations. We simulated $\Delta\sigma$ and V_{oc} for different light intensities. In these simulations, the measured spectra of a T/T2 flash lamp were used (see Table 1). We applied the new method, outlined in the previous section, to the simulated data in order to calculate $\mu_{sum}(\Delta n)$. The calculated $\mu_{sum}(\Delta n)$ was then compared with the μ_{sum} used as input in PC-1D to demonstrate the accuracy of our method. Note that the mobility model used in PC-1D is *not* injection level dependent; only a temperature-, doping- and field-dependent model or fixed values can be used.

Table 1: PC-1D parameters used to demonstrate the validity of the new mobility measurement method.

Spectrum	Experimental data from Qflash T/T2 and diffusing UV filter QF64 from Quantum Instruments [11].
Optics	100 nm thick ARC with $n = 1.46$ Internal $R_{front} = 10\%$, specular Internal $R_{rear} = 10\%$, specular
Bulk	200 μm thick $N_A = 1.513 \times 10^{16} \text{ cm}^{-3}$ (1 Ωcm) $\tau_{n0} = \tau_{p0} = 604.8 \mu\text{s}$, $E_r E_i = 0$ $\Rightarrow \tau_{LLI} = 550 \mu\text{s}$ ($L_{LLI} = 1215 \mu\text{m}$) $\mu_n = 1040 \text{ cm}^2/\text{Vs}$, $\mu_p = 412.6 \text{ cm}^2/\text{Vs}$ (fixed, field independent) $n_i = 1.00 \times 10^{10} \text{ cm}^{-3}$ at 300 K
n^+ emitter	$N_s = 5 \times 10^{18} \text{ cm}^{-3}$, $x_{depth} = 0.1 \mu\text{m}$, Gaussian $\Rightarrow x_{junction} = 0.241 \mu\text{m}$, $R_{sh} = 135.5 \Omega/\text{sq}$. $S_{n0} = S_{p0} = 100 \text{ cm/s}$
p^+ BSF	$N_s = 5 \times 10^{18} \text{ cm}^{-3}$, $x_{depth} = 0.1 \mu\text{m}$, Gaussian $\Rightarrow x_{junction} = 0.241 \mu\text{m}$, $R_{sh} = 341.6 \Omega/\text{sq}$. $S_{n0} = S_{p0} = 100 \text{ cm/s}$

PC-1D simulations were performed for light intensities between 0.001 and 1000 Suns. Figure 1 shows $\Delta\sigma$ versus the incident light intensity ϕ_L . The relation between ϕ_L and $\Delta\sigma$ is given in equation (3) considering the QSS condition and equation (1). This relation is linear for low injection levels (inset in Figure 1) and non-linear in the intermediate and high injection range due to the decreasing

Auger lifetime. Note that the non-linear increase of ϕ_L with increasing $\Delta\sigma$ would be even more pronounced if we chose an injection level dependent mobility model.

$$\phi_L \propto \frac{\Delta n}{\tau_{eff}} \propto \frac{\Delta\sigma}{\tau_{eff}(\mu_n + \mu_p)}, \quad (3)$$

Figure 2 shows the simulated split of the quasi-Fermi energies $E_{Fn}-E_{Fp}$ versus ϕ_L . We expect that the quasi-Fermi energies are constant throughout the entire device. In this case the maximum split of $E_{Fn}-E_{Fp}$ (open circles in Figure 2) is equal to V_{oc} (filled circles in Figure 2), which corresponds to the difference of E_{Fn} and E_{Fp} at the two external terminals. Agreement of both lines in Figure 2 demonstrates that this condition is fulfilled for almost the entire injection range.

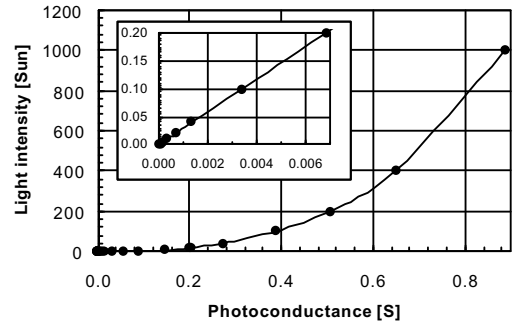


Figure 1: Simulated photoconductance versus light intensity for the device of Table 1.

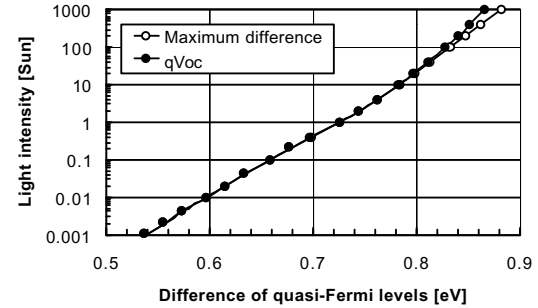


Figure 2: Simulated difference of the quasi-Fermi levels versus light intensity for the device of Table 1. Shown are the maximum splitting (open circles) and the difference between the external contacts (filled circles).

Figure 3 presents $\mu_{sum}(\Delta n_{av})$ as calculated with equation (1) using different ways to calculate Δn_{av} . At low electric fields, PC-1D gives $\mu_{sum} = 1452.6 \text{ cm}^2/\text{Vs}$ per default at a doping density N_{Bulk} of $1.513 \times 10^{16} \text{ cm}^{-3}$. This value is shown as solid line in Figure 3 and was used for the simulations shown in Figure 1 and Figure 2.

Furthermore, the average excess carrier density Δn_{av} was obtained from the simulations by taking the average of $\Delta n(x)$ over the whole solar cell. The simulated $\Delta\sigma-\Delta n_{av}$ data were then used to calculate $\mu_{sum}(\Delta n_{av})$ using equation (1) and are presented as filled circles in Figure 3. These calculations agree excellently with the simulation input of μ_{sum} (solid line) over the entire injection range, demonstrating that our new mobility measurement

approach works, at least as long as Δn_{av} can be measured.

Using equation (2) to calculate $\Delta n_{av} = \Delta n_{scr}$ from the simulated V_{oc} values of Figure 2, we obtain $\mu_{sum}(\Delta n_{av})$ shown in Figure 3 as open circles. Good agreement between this calculation and the simulation input of μ_{sum} (solid line) can be observed for injection levels above 10^{14} cm^{-3} . However, at injection levels below 10^{14} cm^{-3} , μ_{sum} is significantly overestimated by using the described method. This is because $\Delta n_{av} \approx \Delta n_{scr}$ does not hold for very low injection levels as described in Ref. 10.

The filled squares in Figure 3 present $\mu_{sum}(\Delta n_{av})$ calculated from the simulated $\Delta\sigma - \Delta n_{av}$ relation using the field-dependent mobility model in PC-1D. For very low injection levels (where the approximation $\Delta n_{av} = \Delta n_{scr}$ is not valid) $\mu_{sum}(\Delta n_{av})$ decreases due to its field-dependence in the space-charge region. The open squares in Figure 3 present $\mu_{sum}(\Delta n_{av})$ calculated from the simulated $\Delta\sigma - V_{oc}$ relation using the field-dependent mobility model in PC-1D. Due to the decreasing mobility in the space-charge region, this curve has smaller mobility values than the corresponding curve where fixed mobilities were used (open circles).

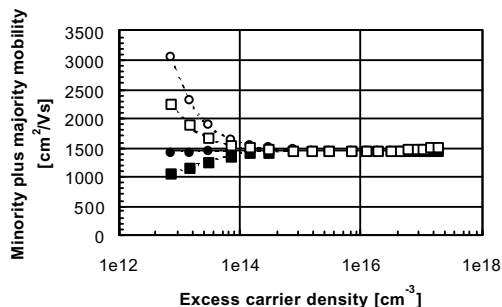


Figure 3: Sum of the minority and majority carrier mobilities versus excess carrier density calculated from $\Delta\sigma - \Delta n_{av}$ (filled circles) and $\Delta\sigma - \Delta n_{scr}$ (open circles) using the fixed input μ_{sum} in PC-1D and calculated from $\Delta\sigma - \Delta n_{av}$ (filled squares) and $\Delta\sigma - \Delta n_{scr}$ (open squares) using the field-dependent mobility model in PC-1D. The solid line presents the fixed mobility $\mu_{sum} = 1452.6 \text{ cm}^2/\text{Vs}$.

4. EXPERIMENTAL VALIDATION OF THE METHOD

We applied our method to measure $\mu_{sum}(\Delta n)$ in the bulk of a PERL Si solar cell, whose structure and fabrication is described in [7]. The cell was processed from a $450(3) \mu\text{m}$ thick p -type FZ Si wafer. We determined its resistivity as $0.96(3) \Omega\text{cm}$ with a four-point-probe measurement, after etching off the emitter and the rear point contacts of the solar cell in KOH. According to the $\sigma - N_{dop}$ relation of Thurber *et al.* [12], this resistivity corresponds to $N_{bulk} = 1.52(6) \times 10^{16} \text{ cm}^{-3}$. The metal was removed from the cell to be able to measure the photoconductance via inductive coupling. However, to avoid Schottky barrier formation at high injection levels, we did not remove the front and rear metal in a small region of the cell outside the region, where the photoconductance is inductively measured.

For the QSS measurement of both V_{oc} and $\Delta\sigma$ versus ϕ_L , we used a commercial photoconductance measurement

system [11] consisting of a flash lamp (Qflash X/X2 and two diffusing UV filters QF64 from Quantum Instruments with a very similar spectrum to the Qflash T/T2 used in our simulations), a bridge circuit, a calibrated reference solar cell, and a two-channel oscilloscope (Tektronix TDS 210). For the conductance calibration of the bridge we used calibrated Si wafers of different conductivity. Note that it would have been sufficient to record $\Delta\sigma - V_{oc}$. However, in order to reduce noise, the $\phi_L - V_{oc}$ and $\phi_L - \Delta\sigma$ relation were recorded separately.

Figures 4 and 5 show the $\phi_L - \Delta\sigma$ and $\phi_L - V_{oc}$ relations, respectively, measured on a PERL cell. The insets in both figures present the corresponding oscilloscope output, from which the main graphs were calculated. To cover a wide injection range, similar measurements were performed for various flash intensity ranges by varying the distance between the flash and the sample.

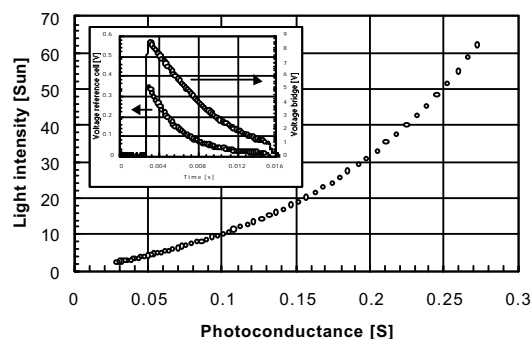


Figure 4: Measured light intensity versus photoconductance of the PERL cell. The inset shows the oscilloscope trace of the reference solar cell voltage and the bridge voltage versus time from which the main graph was calculated.

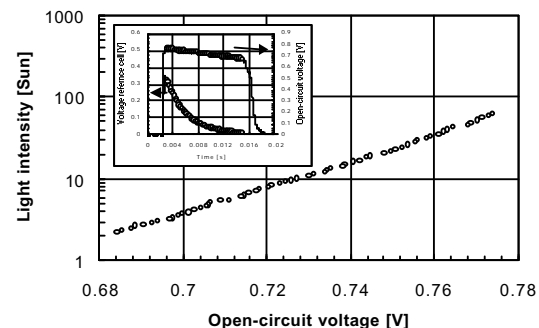


Figure 5: Measured light intensity versus open-circuit voltage of the PERL cell. The inset shows the oscilloscope trace of the reference solar cell voltage and the open-circuit voltage versus time from which the main graph was calculated.

We used equation (1) and (2) to calculate $\mu_{sum}(\Delta n)$ from the $\phi_L - V_{oc}$ and $\phi_L - \Delta\sigma$ data. The results are shown as open circles in Figure 6. We assumed $\Delta n_{av} = \Delta n_{scr}$ for the PERL solar cell because of its good surface passivation properties. The accuracy of determining Δn_{scr} was strongly improved by monitoring the temperature of the wafer with a thermistor circuit and considering the strong temperature dependence of $n_{i,eff}$ [13] in our analysis. In our case the temperature in the wafer was 304.4 K due to heating from

the transformer of the bridge circuit. Furthermore, we calculated $n_{i,eff}$ as a function of dopant density, injection level and temperature with the bandgap narrowing (BGN) model of Ref. 14. This was important, as it reduced μ_{sum} by about 20% for our bulk doping density and injection range.

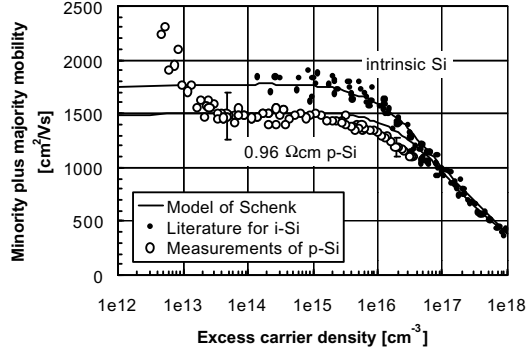


Figure 6: Experimental injection level dependence of the sum of the minority and majority carrier mobilities of $1.52 \times 10^{16} \text{ cm}^{-3}$ p-Si (open circles). Data from the literature [15-17] for intrinsic Si are shown as filled dots. The solid lines were calculated using a quantum-mechanical model [4].

Similar to our PC-1D simulations, our experimental $\mu_{sum}(\Delta n_{av})$ is overestimated at very low injection densities ($< 4 \times 10^{13} \text{ cm}^{-3}$) described in Ref. 10. We also added literature data [15-17] for intrinsic Si in Figure 6 (filled dots). The solid lines in Figure 6 presents $\mu_{sum}(\Delta n_{av})$ calculated with the quantum-mechanical mobility model of Ref. 4, generalised for medium- and high-injection conditions. The parameterisation of $\mu_{sum}(\Delta n)$, used so far in QSS lifetime-measurements [5] agrees with the quantum-mechanical model very well. This quantum-mechanical model describes our experimental data very precisely, except above $\Delta n_{av} = 4 \times 10^{15} \text{ cm}^{-3}$. PC-1D simulations for these conditions ($\Delta n_{av} > 4 \times 10^{15} \text{ cm}^{-3}$, $W = 450 \mu\text{m}$ and spectra of our flash lamp) show that the approximation $\Delta n_{av} = \Delta n_{scr}$ slightly overestimates Δn_{av} . Consequently, $\mu_{sum}(\Delta n_{av})$ is slightly underestimated in this injection range. The physical reason for this is that at high injection levels the diffusion length is Auger-limited and it becomes smaller than the device thickness. However, this limitation could be overcome by the use of thinner wafers. An additional deviation may be due to the fact that $\mu_{sum}(\Delta n)$ is limited by electron-hole scattering in this injection range, which was theoretically derived using the Born approximation. The latter fails if the free carriers are slowed down considerably by scattering, which may happen at $\Delta n_{av} > 4 \times 10^{15} \text{ cm}^{-3}$.

Our estimated absolute error is 0.7% in W , 3.9% in N_{Bulk} , 0.1% in T , 0.2% in V_{oc} , and 0.2% in $\Delta\sigma$, respectively. This results in the absolute errors shown in Figure 6, decreasing from 200 cm^2/Vs in low injection to 50 cm^2/Vs in high injection assuming that $\Delta n_{av} = \Delta n_{scr}$ is satisfied. We found that the error in V_{oc} has the largest impact on the uncertainty of μ_{sum} . This offers the possibility for improving the precision of the method by using a 12-bit data acquisition card with greater accuracy than the present oscilloscope).

5. CONCLUSIONS

We developed a simple technique to measure the injection level dependence of the sum of the minority and majority carrier mobilities $\mu_{sum}(\Delta n_{av})$ in the bulk region of solid-state solar cells. Our experimental set-up is widely used for excess carrier lifetime measurements on Si solar cells. After verifying our method with PC-1D simulations, we measured $\mu_{sum}(\Delta n_{av})$ of a solar cell with a bulk doping of $N_{Bulk} = 1.52(6) \times 10^{16} \text{ cm}^{-3}$. To our knowledge, this is the first time that $\mu_{sum}(\Delta n_{av})$ has been determined from low- to medium- to high-injection levels. Our measurements generally confirm quantum-mechanical calculations, which agree with the parameterisation of $\mu_{sum}(\Delta n_{av})$, used so far in QSS lifetime-measurements in c-Si. However, our method enables the measurement of $\mu_{sum}(\Delta n_{av})$ for other materials where μ_{sum} is insufficiently known such as multi-crystalline Si, or other semiconductors. This makes the proposed method a powerful tool in conjunction with QSS lifetime measurements.

ACKNOWLEDGMENTS

DHN acknowledges a Postgraduate Scholarship and an International Postgraduate Research Scholarship provided by the Centre for Photovoltaic Engineering and the University of New South Wales, respectively. PPA was funded by the Australian Research Council. Many thanks to J. Zhao and X. Dai for their help with sample preparation. We are grateful to A. Afshin of the NREL in Golden, USA for measuring the spectra of the flash lamp. DHN acknowledges N.-P. Harder and T. Trupke for helpful discussions. The Centre for Photovoltaic Engineering has been supported under the Australian Research Council's Centres Scheme.

REFERENCES

- 1 R.A. Sinton and A. Cuevas, Appl. Phys. Lett. **69**, 2510 (1996).
- 2 R.A. Sinton and A. Cuevas, 16th EC PVSEC, 1152 (2000).
- 3 J.M. Dorkel and P. Leturcq, Solid-State Electr. **24**, 821 (1981).
- 4 A. Schenk, J. Appl. Phys. **79**, 814 (1996).
- 5 P.P. Altermatt *et al.*, 16th EU PVSEC, 243 (2000).
- 6 P.A. Basore, IEEE Trans. Elec. Dev. **37**, 337(1990).
- 7 A. Wang *et al.*, J. Appl. Phys. **57**, 602 (1990).
- 8 P.P. Altermatt *et al.*, Tech. Digest 11th PVSEC, 719(1999).
- 9 A. Cuevas and R.A. Sinton, Prog. Photov. **5**, 79 (1997).
- 10 D.H. Neuhaus and A.G. Aberle (to be published).
- 11 Sinton Consulting Inc., 1132 Green Circle, Boulder, CO USA 80303, USA.
- 12 W.R. Thurber *et al.*, J. Electrochem. Soc. **127**, 1807(1980).
- 13 M.A. Green, J. Appl. Phys. **67**, 2944 (1990).
- 14 A. Schenk, J. Appl. Phys. **84**, 3684 (1998).
- 15 F. Dannhäuser, Solid-State Electron. **15**, 1371 (1972).
- 16 J. Krause, Solid-State Electron. **15**, 1377 (1972).
- 17 V. Grivitskas *et al.*, Solid-State Electron. **27**, 565 (1984).